JACS
JOURNAL OF THE AMERICAN CHEMICAL SOCIETY
Article
pubs.acs.org/JACS

Structure and Function of a Bacterial Microcompartment Shell Protein Engineered to Bind a [4Fe-4S] Cluster

Clément Aussignargues,[†] Maria-Eirini Pandelia,[‡,∞] Markus Sutter,[†,§] Jefferson S. Plegaria,[†] Jan Zarzycki,[†,◆] Aiko Turmo,[†] Jingcheng Huang,[†,¶] Daniel C. Ducat,[†,¶] Eric L. Hegg,[¶] Brian R. Gibney,[#,∥] and Cheryl A. Kerfeld*[,†,§,¶,⊥,▽]

[†]MSU-DOE Plant Research Laboratory and [¶]Department of Biochemistry & Molecular Biology, Michigan State University, East Lansing, Michigan 48824, United States

[‡]Department of Chemistry, The Pennsylvania State University, University Park, Pennsylvania 16802, United States

[§]Physical Biosciences Division, Lawrence Berkeley National Laboratory, Berkeley, California 94720, United States

[#]Department of Chemistry, Brooklyn College, Brooklyn, New York 11210, United States

[∥]Ph.D. Programs in Chemistry and Biochemistry, The Graduate Center of the City University of New York, New York, New York 10016, United States

[⊥]Department of Plant and Microbial Biology, University of California, Berkeley, California 94720, United States

[▽]Berkeley Synthetic Biology Institute, Berkeley, California 94720, United States

Supporting Information

ABSTRACT: Bacterial microcompartments (BMCs) are self-assembling organelles composed of a selectively permeable protein shell and encapsulated enzymes. They are considered promising templates for the engineering of designed bionanoreactors for biotechnology. In particular, encapsulation of oxidoreductive reactions requiring electron transfer between the lumen of the BMC and the cytosol relies on the ability to conduct electrons across the shell. We determined the crystal structure of a component protein of a synthetic BMC shell, which informed the rational design of a [4Fe-4S] cluster-binding site in its pore. We also solved the structure of the [4Fe-4S] cluster-bound, engineered protein to 1.8 Å resolution, providing the first structure of a BMC shell protein containing a metal center. The [4Fe-4S] cluster was characterized by optical and EPR spectroscopies; it has a reduction potential of −370 mV vs the standard hydrogen electrode (SHE) and is stable through redox cycling. This remarkable stability may be attributable to the hydrogen-bonding network provided by the main chain of the protein scaffold. The properties of the [4Fe-4S] cluster resemble those in low-potential bacterial ferredoxins, while its ligation to three cysteine residues is reminiscent of enzymes such as aconitase and radical *S*-adenosymethionine (SAM) enzymes. This engineered shell protein provides the foundation for conferring electron-transfer functionality to BMC shells.

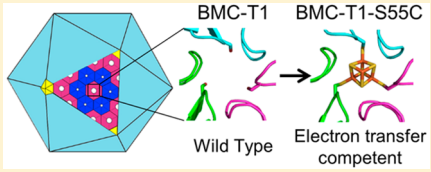

INTRODUCTION

Bacterial microcompartments (BMCs) are polyhedral organelles (typically 40−200 nm in diameter) consisting of a proteinaceous shell that encloses a multienzyme core (recently reviewed in refs 1 and 2). While all BMCs share an architecturally similar shell, the encapsulated enzymes vary, contributing to the remarkable functional and phylogenetic diversity of BMCs.[3] The BMC shell comprises three different types of proteins that serve as its basic building blocks (Figure 1). BMC-H subunits (single Pfam00936 domain) assemble into a cyclic hexamer. Tandem (BMC-T) proteins consist of a fusion of two Pfam00936 domains; BMC-T trimers form a pseudohexamer.[4,5] BMC-P proteins (single Pfam03319 domain) assemble into pentamers that cap the vertices of an apparently icosahedral shell (Figure 1).[6−8] The shell protein oligomers typically contain pores at the symmetry axis that are proposed to function as selective conduits for the diffusion of metabolites (substrates and products) into and out of the BMC lumen.[9,10]

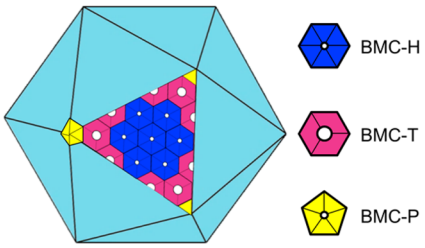

Figure 1. BMC shell organization. Schematic of the composition of a BMC shell. For clarity, only one facet of the icosahedron is tiled with shell proteins.

Received: November 9, 2015
Published: December 24, 2015

DOI: 10.1021/jacs.5b11734
J. Am. Chem. Soc. 2016, 138, 5262−5270

Given their attributes as self-assembling and selectively permeable organelles, BMCs have attracted intense interest as design templates for the engineering of subcellular bionanoreactors that can be customized to support new metabolic functions.[1,11] Toward this aim, non-native proteins have been encapsulated into shells.[12−15] However, successful utilization of encapsulated pathways is predicated on engineering the shell to allow selective flux of substrates and products. To sustain encapsulated oxidoreductive reactions, it would be ideal to be able to conduct electrons from the cytosol into the BMC or, conversely, to be able to "evacuate" electrons from the encapsulated metabolism. For these aims, introduction of an electron-transfer competent cofactor into the shell is imperative. There is evidence that suggests that electron-transport competent shell proteins are found in some BMCs[12,16] for which a [4Fe-4S] cluster-binding site has been proposed.[17,18] Yet, to date there has been only solution-state biophysical characterization of presumed [4Fe-4S] cluster-binding shell proteins;[12] crystal structures for interpreting the properties of the presumed clusters are lacking.

[Fe-S] clusters are one of the most ubiquitous cofactors in nature and are widespread among organisms from all three domains of life.[19] Their structural and redox plasticity encompasses a diverse functional repertoire, ranging from electron transfer, nonredox and redox catalysis, O_2-sensing, and structural roles.[20] This functional diversity is supported by distinct types of clusters ([2Fe-2S], [3Fe-4S], [4Fe-4S] clusters being the most common ones) and by their ability to access a wide range of reduction potentials (i.e., between −600 mV and +450 mV).[21] Because of this extraordinary versatility, [Fe-S] clusters are of considerable interest for metalloprotein design. Here we describe the successful engineering of a BMC shell protein to incorporate a [4Fe-4S] cluster and its spectroscopic characterization. We structurally characterized a BMC-T shell protein (BMC-T1) from a synthetic BMC shell system (HO shell).[14] Based on the structure, we designed a [4Fe-4S] cluster-binding site at the three-fold symmetry axis of the trimer. We determined the crystal structure of this engineered variant (BMC-T1-S55C) to 1.8 Å resolution and verified the incorporation of a [4Fe-4S] cluster in its pore. We characterized the [4Fe-4S] cluster of BMC-T1-S55C by spectroscopic methods (optical and EPR) and demonstrated that the cluster is redox active, with a reduction potential of −370 mV vs SHE. The cluster remains intact upon successive redox cycles, poising the engineered shell protein to serve as an interface between the BMC lumen and the redox status of the cytosol. This is the first time a new function, specifically electron transfer, has been introduced into a BMC shell protein. BMC-T1-S55C also represents the first structure of a designed [4Fe-4S] cluster protein. This work is a major step toward constructing synthetic BMCs that can transfer electrons and encapsulate oxidoreductive pathways for biotechnological applications.

EXPERIMENTAL SECTION

Plasmids, Bacterial Strains, and Growth Conditions. The gene coding for BMC-T1 was subcloned in a pET11 plasmid DNA vector from the previously described DNA construct[14] that codes for the seven shell proteins of the synthetic shells. The S55C amino acid substitution was introduced in the *hoch_5812* gene using the QuikChange Lightning site-directed mutagenesis kit (Agilent Technologies) using the instructions provided by the manufacturer. The plasmids containing the sequence coding for BMC-T1 (pCA14) and BMC-T1-S55C (pCA15) were transformed in *Escherichia coli* BL21 (DE3) for heterologous expression.

For aerobic expression of BMC-T1, the corresponding recombinant *E. coli* strain was grown in LB broth (Miller) with 100 mg·L^{-1} ampicillin at 37 °C with agitation (160 rpm) to $OD_{600\ nm}$ = 0.6, then induced with 0.45 mM isopropyl thio-β-D-thiogalactoside (IPTG) and grown for another 15 h at 22 °C. The cells were then harvested and stored at −80 °C.

The anaerobic expression of BMC-T1-S55C was performed by a modified protocol from Kuchenreuther et al.[22] Cultures were grown in a MOPS/NaOH buffered (100 mM, pH 7.5) LB medium. First, bottles containing MOPS buffer were sparged with nitrogen gas to remove oxygen. The bottles were capped (using rubber caps) and transferred into an anaerobic chamber (Coy, Grass Lake, Michigan). The buffer was then supplemented with LB broth (Miller) granulates (EMD Millipore). The bottles were sealed with rubber stoppers and autoclaved. The sterile media bottles were then anaerobically supplemented with 25 mM glucose, 25 mM sodium fumarate, 1 mM L-cysteine, 1 mM ferric ammonium citrate, and 100 mg·L^{-1} ampicillin. The bottles were then inoculated (2% v/v) with an aerobically grown preculture. The anaerobic cultures were grown at 37 °C with agitation (120 rpm). When the cultures reached an $OD_{600\ nm}$ of 1, the culture was induced with 1 mM IPTG and grown for another 20 h at the same temperature. The cells were harvested and stored at −80 °C under anaerobic conditions.

Protein Purification and [Fe-S] Cluster Reconstitution. BMC-T1 was purified as follows: Cells (typically from 1 L *E. coli* culture) were resuspended in 50 mM Tris/HCl pH 7.5, 75 mM NaCl (buffer A) (cell wet weight to buffer volume ratio 1:2) in the presence of DNase and lysed by two consecutive passages through a French Press at a pressure of 137 MPa. This crude lysate was then heated to 55 °C for 30 min to precipitate other proteins (BMC-T1 is relatively stable at this temperature). This step was followed by centrifugation at 8000 *g* for 20 min to pellet the precipitated proteins and cell debris. The supernatant was filtered through a 0.22 μm filter and loaded on a Tosoh Toyopearl SuperQ column equilibrated in buffer A. The protein was eluted using a gradient from 75 to 500 mM NaCl in 10 column volumes. Fractions showing the presence of the protein on SDS-PAGE were pooled and concentrated using an Amicon centrifugal concentrator (30 kDa cutoff). The protein was then applied to a gel filtration column (HiLoad 16/600 Superdex 75 pg, GE Healthcare) and equilibrated with a 50 mM Tris/HCl pH 7.5, 150 mM NaCl buffer. The purified proteins were then stored at 4 °C. Purified BMC-T1 was buffer-exchanged to 10 mM Tris/HCl pH 7.5 using a PD-10 column (GE Healthcare) and concentrated to 5.5 mg·ml^{-1} for crystallization.

BMC-T1-S55C was purified as described above in an anaerobic chamber, typically from a 6 L anaerobic *E. coli* culture and using a MOPS/NaOH buffer system instead of Tris/HCl. Buffers used for the purification were degassed and allowed to equilibrate with the anaerobic chamber atmosphere (95% N_2, 5% H_2) for at least 1 day prior to use. After anion exchange chromatography, the sample was subjected to [Fe-S] cluster reconstitution under anaerobic conditions: The diluted protein was incubated with 10 mM DTT for 1 h at 4 °C, then $FeCl_3$ was added to a final concentration of 400 μM and followed by a 3−4 h incubation at 4 °C. Finally, the same concentration of Na_2S was added, and the sample was incubated at 4 °C overnight, before being concentrated, filtered, and purified using gel filtration. For crystallization experiments, reconstituted BMC-T1-S55C was buffer-exchanged to 10 mM MOPS/NaOH pH 7.5, 10 mM NaCl, 10 mM DTT, and concentrated to 8.5 mg·ml^{-1}.

Protein concentrations were determined using the bicinchoninic acid (BCA) kit (Sigma-Aldrich). Iron content was determined by the ferrozine method.[23]

Crystallization and Structure Determination. BMC-T1 crystals were obtained by mixing 2 μL of protein with an equal volume of a reservoir solution containing 30 mM citric acid/70 mM bis-Tris propane (final pH 7.6) and 18% PEG 3,350 in sitting drop trays. Crystals were cryoprotected using PEG 400 at a final concentration of 25%. BMC-T1-S55C crystals were grown in sitting drops using 250

DOI: 10.1021/jacs.5b11734
J. Am. Chem. Soc. 2016, 138, 5262−5270

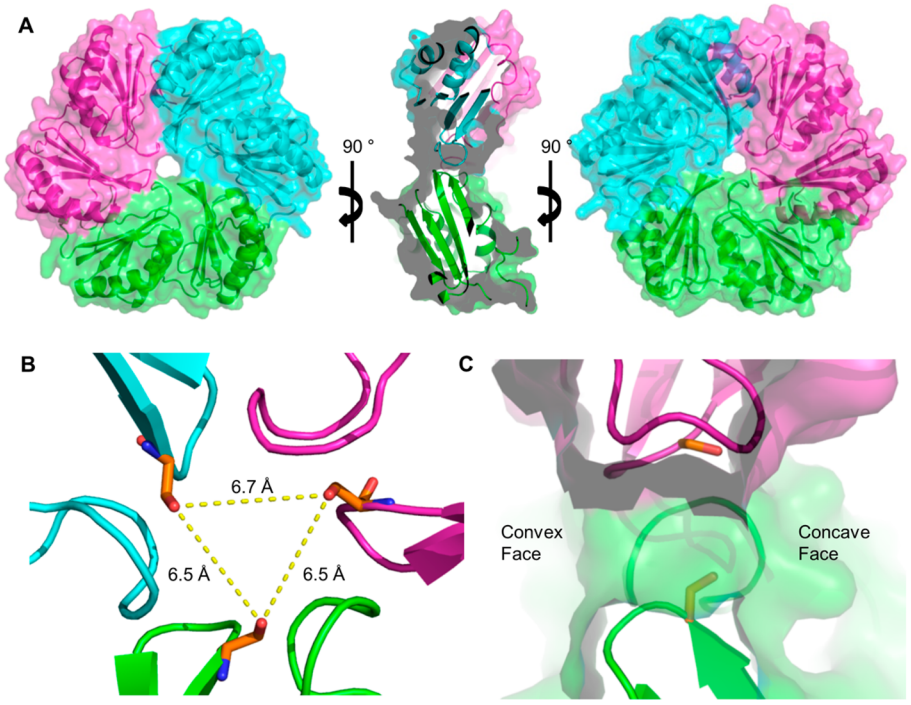

Figure 2. Structure of BMC-T1. (A) Structure of BMC-T1 in three orientations. The convex face of the trimer is shown on the left, the concave side on the right. Each protomer is represented in a different color. (B) O_γ–O_γ trigonal distances between the side chains of the Ser55 residues converging at the three-fold symmetry axis (pore). (C) Side view of the pore region, showing the orientation of the side chains of the Ser55 residues (orange sticks) toward the concave face.

mM sodium acetate, 100 mM Tris/HCl pH 8.5, 26% PEG 4000 as reservoir condition (protein/reservoir ratio of 1:1). Cryoprotection was achieved using 38% 1,2-propanediol and 21% MPD (final concentrations). Stabilized crystals were flash frozen in liquid nitrogen until data collection. For BMC-T1-S55C, all steps (except looping and freezing steps) were conducted in a Coy anaerobic chamber. X-ray diffraction data were collected at beamline 12-2 (100 K, 0.977408 Å wavelength) of the Stanford Synchrotron Radiation Light Source (BMC-T1) and at the Advanced Light Source at Lawrence Berkeley National Laboratory beamline 5.0.3 (BMC-T1-S55C, 100 K, 1.0000 Å wavelength). Diffraction data were integrated with XDS[24] and scaled with SCALA (CCP4).[25] The BMC-T1 structure was solved by molecular replacement with Phaser[26] using a carboxysome BMC-T protein, CsoS1D from *Prochlorococcus marinus* (PDB ID: 3FCH) as the search model. Autobuilding was performed using phenix.autobuild[27] followed by cycles of manual rebuilding in COOT[28] and refinement with phenix.refine,[27] which also performed the automatic water picking. The structure of BMC-T1-S55C was solved using molecular replacement with the structure of BMC-T1. Statistics for diffraction data collection, structure determination, and refinement are summarized in Table S1. The final model had 93.8% and 95.9% of the residues in the favored, 6.1% and 3.9% in the allowed, and 0.1% and 0.2% in the disallowed region of the Ramachandran plot for BMC-T1 and BMC-T1-S55C, respectively. Figures of structural models were prepared using PyMOL (www.pymol.org). Atomic coordinates and structure factors (PDB ID: 5DIH for BMC-T1 and 5DII for BMC-T1-S55C) have been deposited in the Protein Data Bank [http://www.pdb.org/].

Optical Spectroscopy. UV–visible (UV–Vis) spectra were recorded in anaerobic conditions using an Agilent Technologies Cary60 UV–vis spectrophotometer. For reduction tests, proteins (in 50 mM MOPS/NaOH pH 7.5, 75 mM NaCl) were mixed in anaerobic conditions with 0.5 mM sodium dithionite and incubated for 5–10 min before recording the spectra.

Electron Paramagnetic Resonance (EPR). Continuous wave EPR experiments at variable temperatures (5–70 K) were carried out at a Bruker ESP300 spectrometer equipped with a continuous flow cryostat (Oxford Instruments) and a Bruker ER/4102 ST rectangular resonator which operates in the TE_{102} (9.48 GHz) perpendicular mode. The microwave frequency was measured with a 5350B Hewlett Packard frequency counter. For all experiments, custom-made quartz tubes of the same inner and outer diameter were used (QSI). Quantitation of the signals was carried out by measuring a 256 μM Cu^{2+}-EDTA standard under nonsaturating conditions by double numerical integration of the first-derivative experimental and simulated EPR spectra. All quantitations were carried out for the spectra recorded at T = 10 K. The first-derivative EPR spectra were simulated using the MATLAB (Mathworks) based Easyspin simulation software.[29] The samples were transferred to the EPR tubes under anaerobic conditions and were quickly frozen in liquid nitrogen in a Coy anaerobic chamber prior to measuring.

Redox Potentiometry. Chemical redox titrations were performed as described by Dutton,[30] and all values are reported relative to the SHE. Titrations were performed in aqueous solutions containing 60 μM iron-sulfur cluster protein in 50 mM MOPS/NaOH pH 7.5, 75 mM NaCl with the following mediators: anthraquinone-2,6-disulfonate (0.6 μM), anthraquinone-2-sulfonate (0.6 μM), benzyl viologen (0.2 μM), and methyl viologen (0.2 μM). Reduction was accomplished with sodium dithionite and re-oxidation with duroquinone. The normalized absorbance change at 422 nm (selected to eliminate the contribution of the viologen dyes) due to [4Fe-4S] cluster reduction was fitted to an N = 1 Nernst equation.

RESULTS

Structural Characterization of BMC-T1. Synthetic HO shells[14] are derived from a BMC of unknown function[3] encoded in the genome of the myxobacterium *Haliangium ochraceum*. They are composed of seven gene products; four (BMC-T1-T3 and one BMC-H protein) are components of the facets of the shell[14] (Figure 1). We chose BMC-T1 (locus tag: Hoch_5812) for characterization and as a scaffold for the incorporation of a metal center because it was predicted to form trimers that incorporate into single-layered facets of the

DOI: 10.1021/jacs.5b11734
J. Am. Chem. Soc. 2016, 138, 5262–5270

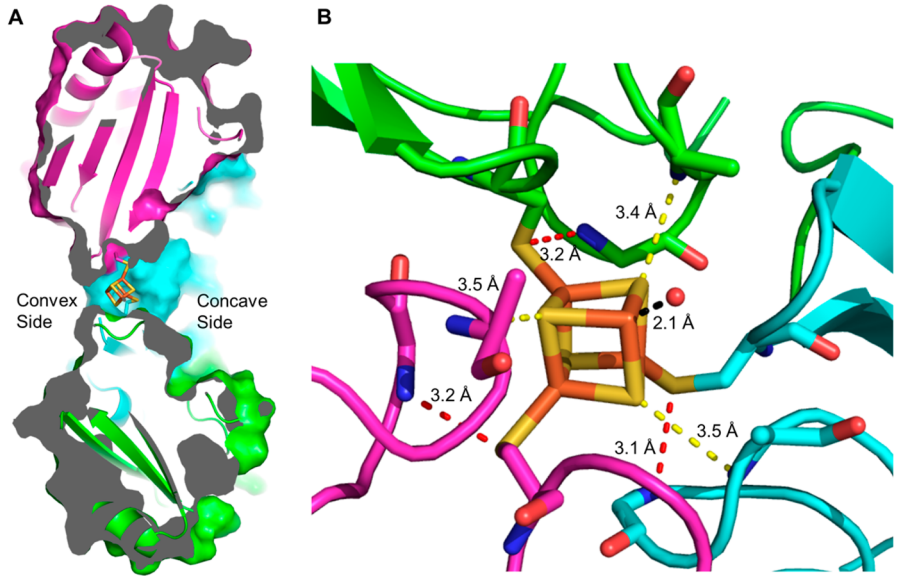

Figure 3. Structure of BMC-T1-S55C. (A) Side view of the structure showing the [4Fe-4S] cluster (yellow and orange sticks). (B) Zoomed in view of the three-fold symmetry axis (pore region) showing the [4Fe-4S] cluster with the water molecule (red sphere) as the fourth unique iron ligand (black dashed line). Red dashed lines represent hydrogen bonds between the backbone amide of Gly155 and the sulfur atom of Cys55, while yellow dashed lines represent hydrogen bonds between the backbone amide of Ala157 and the cluster sulfides.

synthetic shell.[14] Notably, HO shell proteins are only distantly related to their counterparts in experimentally characterized BMCs (e.g., the propanediol utilization and ethanolamine utilization BMCs and the carboxysome). For example, a BLAST search of the nonredundant sequence database indicates that the closest homologue of BMC-T1 is a BMC-T protein encoded in the genome of *Hyalangium minutum* (which also belongs to the *Myxococcales*) with 49% identity. The next closest homologues share only 37% identity or less with BMC-T1. In a query of the Protein Data Bank (PDB), three hits, each 36% identical at the level of primary structure, were returned: PduT, a BMC-T protein of the propanediol utilization BMC of *Salmonella enterica* (PDB ID 3N79) and *Citrobacter freundii* (PDB ID 3PAC) as well as a homologue from a glycyl radical enzyme-associated BMC[3] identified in *Desulfitobacterium hafniense* (PDB ID 3NWG). Given this relatively remote sequence homology to structurally characterized BMC shell proteins, we determined the structure of BMC-T1 wild-type (WT) to guide the design of a [4Fe-4S] cluster-binding site.

The protein was overexpressed in *E. coli*, and the purified protein crystallized in the monoclinic space group $P2_1$. The crystals diffracted to a resolution of 2.4 Å (Table S1), and the structure was solved by molecular replacement using CsoS1D from *Prochlorococcus marinus* (PDB ID: 3FCH) as the search model. There were six subunits (two trimers) per asymmetric unit; the trimer structure is shown Figure 2A. Due to disordered termini and loops, varying numbers of amino acids (between 3 and 23 residues per chain) had to be omitted from the N-termini and some loop regions of the three monomers. Data collection and refinement statistics are provided in Table S1.

Structure-Based Rational Design of a [4Fe-4S] Cluster-Binding Site into BMC-T1. The structure of BMC-T1 was used to design a [4Fe-4S] cluster-binding site at the cyclic axis of symmetry of the trimer. The hydroxyl side chains of Ser55 from each protomer are arranged in a trigonal plane with O_γ–O_γ distances between 6.46 and 6.74 Å (Figures 2B and S1). This arrangement is reminiscent of the S_γ–S_γ bite distances of cysteine residues coordinating [4Fe-4S] clusters in natural ferredoxins,[31] suggesting that the pore formed at the symmetry of the BMC-T1 trimer could serve as a [4Fe-4S] cluster-binding site. The side chains of the three Ser55 residues (one from each protomer) point toward the concave side of the trimer (Figure 2A,C) and are in a gauche(+) conformation with χ_1 angles of 111–112° (Figure 2B,C). Furthermore, the rigid β-turn motif that contains Ser55 disfavors structural rearrangement to accommodate a rubredoxin-type mononuclear iron that requires a smaller bite distance of 3.8 Å.[31] Given this geometry and bite distance, and taking advantage of the three-fold symmetry axis (pore), we chose to substitute Ser55 with a cysteine to accommodate binding of a [4Fe-4S] cluster (referred to as BMC-T1-S55C).

The Structure of BMC-T1-S55C Confirms Incorporation of a [4Fe-4S] Cluster. Because [4Fe-4S] clusters are typically oxygen sensitive, purification of BMC-T1-S55C was conducted in anaerobic conditions using the same purification protocol as described for the WT protein. In stark contrast to the WT protein that was colorless, purified BMC-T1-S55C exhibited a brown color, suggesting the presence of an [Fe-S] cluster (Figure S2A). Size exclusion chromatography confirmed that BMC-T1-S55C is a trimer (Figure S2B,C).

BMC-T1-S55C was crystallized anaerobically, and the structure was solved at 1.8 Å resolution by molecular replacement using the WT structure as the search model (Table S1). There are two trimers in the asymmetric unit of the *P*1 space group. The electron density was of high quality, with only a few (<6) residues at the N-termini and in some flexible loops (Ala14, Gly15, and Glu116-Thr118) that could not be modeled due to disorder. Both trimers contain electron density that could be readily modeled as a [4Fe-4S] cluster in the middle of the central, positively charged pore (Figures 3A,B and S3 and S4). The electron density is well-defined, and the positions of the iron atoms were confirmed by their anomalous signal (Figures S5 and S6). The occupancy for the [4Fe-4S] cluster was refined to 72–74%. Using the ferrozine assay to measure metal content, we estimate that about 60% of the

DOI: 10.1021/jacs.5b11734
J. Am. Chem. Soc. 2016, 138, 5262–5270

protein contain a [4Fe-4S] cluster, which is consistent with the results of the structure determination. Three of the iron atoms of each cluster are coordinated by the three introduced cysteines (S55C), and a water or hydroxide molecule ligates the fourth unique iron (Figure 3B). The S_γ Cys55−Fe and Fe−OH_2/OH bonds have distances of 2.3 and 2.1 Å, respectively. The Fe−S bonds within the cluster have an average length of 2.2 Å. The Fe−Fe distance is 2.8 Å. These values are comparable to those observed in a variety of [4Fe-4S] cluster proteins and synthetic [4Fe-4S] cluster analogs (Fe−S distances of ∼2.3 Å and Fe−Fe distances of ∼2.5−2.8 Å).[32−35] Moreover, three of the cluster sulfides make hydrogen bonds with the amide backbone of residues Ala157 (of each protomer) with H to S distances of 2.7−2.8 Å (N to S distances of 3.4−3.5 Å) (Figure 3B); these are comparable to main chain-cluster bonds observed in other [4Fe-4S] cluster-containing proteins.[33,36] The sulfur atoms of Cys55 are hydrogen bonded to the backbone amide of Gly155 with S to H distances of 2.1−2.2 Å (S to N distances of 3.1−3.2 Å) (Figure 3B). These hydrogen bonds are also present in the BMC-T1 (WT) structure (amide backbone of Gly155 and O_γ of the Ser55 side chain), demonstrating that the Ser55 to Cys55 mutation did not perturb the overall structure of BMC-T1. This is further corroborated by a structural superposition of BMC-T1 and BMC-T1-S55C (Figure S7); the root-mean-square deviation for 160 α-carbon atom pairs is 0.5 Å. Furthermore, the conformation of the three cysteine residues is conserved with respect to their serine equivalent (χ_1 angle of ∼110°). Overall, the structure validates the original design criteria, and most importantly, it represents the first structure of a designed [4Fe-4S] protein.

Characterization of the [4Fe-4S] Cluster in BMC-T1-S55C by Optical Spectroscopy. The UV−vis spectrum of BMC-T1 does not show any absorbance features other than the 280 nm band of the aromatic residues (Figure 4A). In contrast, after [Fe-S] cluster reconstitution of BMC-T1-S55C, the optical spectrum recorded under anaerobic conditions exhibited a broad absorption band at approximately 385 nm (Figure 4A), which is characteristic of S-to-Fe charge-transfer transitions observed in [Fe-S] cluster-containing proteins.[37,38] In addition, there is no evidence for bands that are typically observed for [2Fe-2S] clusters (features at 310−330, 420, and 465 nm),[38] indicating that the trimer contains exclusively a [4Fe-4S] cluster, as observed in the crystal structure. Treatment with dithionite (−660 mV vs SHE at pH 7)[39] resulted in complete disappearance of the optical features (Figure 4A), consistent with reduction of the cluster. Based on the [4Fe-4S] cluster occupancy in the crystal structure, the extinction coefficient at 385 nm is between 18,000 and 19,000 $M^{-1}\cdot cm^{-1}$, which is within the range reported for other [4Fe-4S] clusters (16,000−23,000 $M^{-1}\cdot cm^{-1}$).[37] Furthermore, similar results were obtained with the nonreconstituted BMC-T1-S55C, although the [4Fe-4S] cluster band was less intense (Figure S8). This indicates a lower efficiency in cluster incorporation; we estimated that about 50% of the protein spontaneously binds a cluster *in vivo*. Enhancement in cluster incorporation by chemical reconstitution is well-known, especially in the case of O_2-sensitive [Fe-S] cofactors or when overexpressing the [Fe-S] containing proteins in the absence of the auxiliary Iron-Sulfur Cluster maturation machinery.[40]

Characterization of the [4Fe-4S] Cluster in BMC-T1-S55C by EPR Spectroscopy. The continuous wave (CW) X-Band EPR spectrum of BMC-T1 (± dithionite) exhibited no

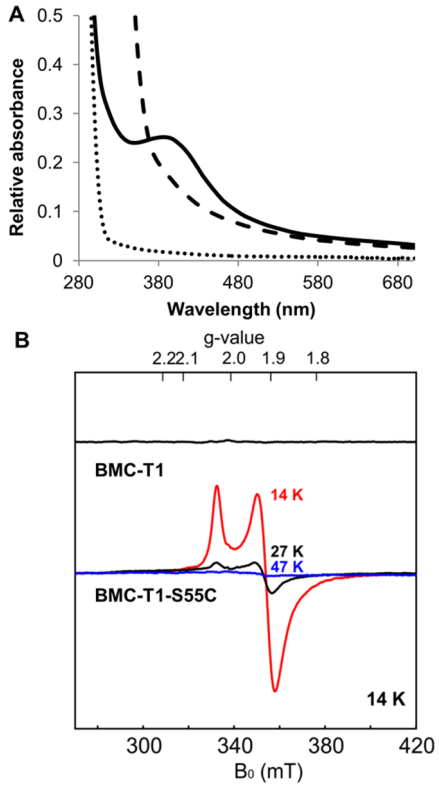

Figure 4. UV−vis and EPR spectra of BMC-T1 and BMC-T1-S55C. (A) UV−vis spectroscopy. Solid line, BMC-T1-S55C as-isolated, after reconstitution. Dashed line, BMC-T1-S55C after reconstitution and incubation with 0.5 mM dithionite. Dotted line, BMC-T1. The spectra were recorded at pH 7.5 and under anaerobic conditions for BMC-T1-S55C. (B) X-Band CW EPR spectra of BMC-T1 (top) and chemically reconstituted BMC-T1-S55C (bottom) after reduction with dithionite. The spectrum of BMC-T1 was recorded at 14 K. The spectra of BMC-T1-S55C were recorded at three different temperatures: 14 K (red trace), 27 K (black trace), and 47 K (blue trace) to demonstrate the relaxation behavior of the $[4Fe\text{-}4S]^{1+}$ signal. Experimental conditions: microwave frequency = 9.481 GHz, microwave power = 0.64 mW, modulation amplitude = 0.6 mT.

paramagnetic signals attributable to [Fe-S] clusters (Figure 4B), which is in agreement with its UV−vis spectrum. In contrast, after reduction with dithionite, both the purified, non-reconstituted, and the chemically reconstituted BMC-T1-S55C proteins exhibited qualitatively comparable EPR spectra that are reminiscent of [4Fe-4S] clusters (Figures 4B and S9 and S10). The degree of [4Fe-4S] cluster incorporation in BMC-T1-S55C was consistently higher in the chemically reconstituted protein than in the nonreconstituted form, which again corroborates the results of the UV−vis analysis. The EPR spectrum of the reconstituted, chemically reduced BMC-T1-S55C was characterized by an axial signal with g_{av} = 1.98 and principal g-values 2.04 and 1.91, respectively. The intensity of this signal was strongly temperature dependent and was barely detectable at temperatures above 45 K (Figure 4B). The effective g-values and the relaxation properties were typical of those reported for $[4Fe\text{-}4S]^{+1}$ clusters with an S = 1/2 ground state.[41] In the case of the nonreconstituted BMC-T1-S55C sample reduced with dithionite, the EPR signal, albeit very similar, exhibited a slight downshift in the low-field g-component, small changes in the rest g-values, and broader line widths (Figure S10). These observations suggest a higher degree of heterogeneity with respect to the reconstituted

DOI: 10.1021/jacs.5b11734
J. Am. Chem. Soc. 2016, 138, 5262−5270

sample, which can be attributed to the formation of clusters in slightly different local protein environments. The EPR signals of the assembled [4Fe-4S] cluster in BMC-T1-S55C varied only marginally between different protein preparations; changes in small *g*-values shifts and overall signal line shape broadness indicate that the incorporated cluster is rather sensitive to local changes in its protein environment (Figure S9). In some cases, an additional low-field signal at $g \sim 2.11$ was detected, suggesting the presence of a second cluster form. After reconstitution, the intensity of this component was markedly reduced, consistent with the suggestion that the [4Fe-4S] cluster incorporated in the chemically reconstituted samples exhibits less heterogeneity (Figure S9). The $g \sim 2.11$ signal may be associated with a different conformation of the [4Fe-4S] cluster, in which the water/hydroxide-ligated iron would be oriented toward the concave face of the trimer instead of being located in the pore or to a different coordination state where the water molecule may be replaced by an inorganic or protein ligand.

To determine if any [3Fe-4S] clusters were present in BMC-T1-S55C, we measured the EPR spectra prior to reduction with dithionite (in both its nonreconstituted and reconstituted forms). No signals attributable to $[3Fe\text{-}4S]^{1+}$ clusters were detected ($g_{av} \sim 2.01$) (Figure S10), thus confirming that only [4Fe-4S] clusters were assembled. In addition, in the reconstituted sample without dithionite, a small amount (about 20% of the total cluster content) of $[4Fe\text{-}4S]^{1+}$ clusters could be observed, suggesting that under these conditions an appreciable fraction of the clusters was partially reduced. Overall, the assembled [4Fe-4S] cluster in BMC-T1-S55C exhibited EPR signals and relaxation properties highly reminiscent of those observed in classical $[4Fe\text{-}4S]^{1+}$ low-potential ferredoxins.

Spectroelectrochemistry of BMC-T1-S55C. The mid-point reduction potential, E_m, of BMC-T1-S55C was determined using UV−vis detected spectroelectrochemistry (Figure 5A). The reduction potential of the [4Fe-4S] cluster in BMC-T1-S55C was determined to be −370 mV vs SHE (±10 mV), which is in agreement with the efficient reduction of the cluster by dithionite. This value also explains the observation of partially reduced clusters after incubation with DTT (−332 mV at pH 7)[42] during the chemical reconstitution of the cluster (Figure S10). Furthermore, reduction of the cluster by dithionite was fully reversible upon addition of duroquinone as an oxidant. Successive reduction/oxidation cycles were repeated without any degradation of the $[4Fe\text{-}4S]^{2+}$ cluster UV−vis signature at ∼385 nm (Figure 5B).

Stability of the [4Fe-4S] Cluster in BMC-T1-S55C upon Chemical Denaturation and Oxygen Exposure. Previous studies have reported that the presence of a cluster can stabilize host proteins.[43] To test this hypothesis in our system, we performed a chemical denaturation monitored by circular dichroism (CD) spectroscopy, using urea, of BMC-T1 and BMC-T1-S55C. Results show that BMC-T1 is fully denatured at 6 M urea; in contrast, BMC-T1-S55C is extremely resistant to chemical denaturation, as very little unfolding was detected, even at concentration of urea as high as 10.2 M (Figure S11). Moreover, the UV−vis spectrum of BMC-T1-S55C in 10.2 M urea exhibits the typical signal at 385 nm (Figure S11). This suggests that BMC-T1-S55C and its [4Fe-4S] cluster are an extremely stable assembly.

We also determined the behavior of the [4Fe-4S] cluster of BMC-T1-S55C toward oxygen. A sample of the anaerobic protein was exposed to air, and UV−vis and EPR spectra (without dithionite) were recorded at different time points (Figure S12). EPR spectra showed that upon exposure to air, a transient $[3Fe\text{-}4S]^{1+}$ cluster is generated, but to only substoichiometric amounts, i.e., 5 μM. In combination with the observations from UV−vis spectroscopy, in which a decrease of the [4Fe-4S] charge-transfer band is relatively fast and accompanied by features that are somewhat reminiscent of [2Fe-2S] clusters, these results demonstrate that the [4Fe-4S] cluster is indeed susceptible to oxidation by dioxygen. This O_2-dependent degradation appears to proceed via a $[3Fe\text{-}4S]^{1+}$ intermediate (by release of one of the Fe) and later formation of an O_2-unstable [2Fe-2S] cluster to its complete degradation after prolonged exposure (several hours to a day). Such a degradation mechanism is not entirely unprecedented, and as previously described, such an oxidative disassembly is strongly linked to the protein environment and the local geometries of the cofactor.[44] Determining a more precise mechanism and the kinetics of the BMC-T1-S55C [4Fe-4S] cluster degradation will be the subject of future studies.

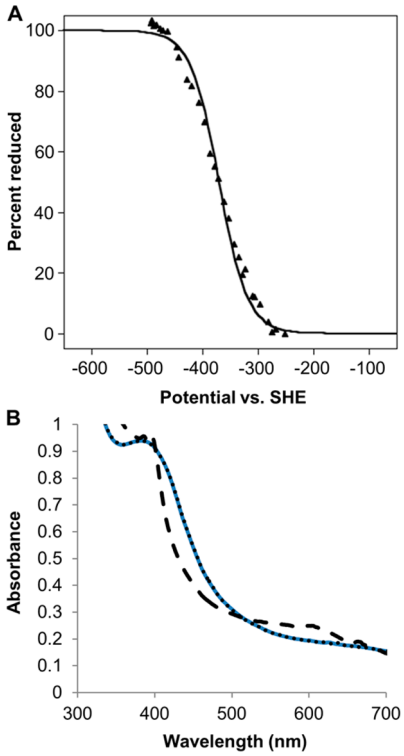

Figure 5. Reduction potential determination of the BMC-T1-S55C [4Fe-4S] cluster by spectroelectrochemistry and redox reversibility. (A) The percentage of reduced protein has been plotted versus the potential and fitted using a single electron Nernst equation. The calculated E_m is −370 mV vs SHE at pH 7.5 and 25 °C. (B) Re-oxidation of the [4Fe-4S] cluster of BMC-T1-S55C after the redox titration. Spectra were recorded before the titration (using dithionite to reduce the cluster, solid blue line), after full reduction (dashed black line), and after re-oxidation using duroquinone (dotted black line). The additional observed signals in the dithionite-reduced spectrum are the contribution of the reduced redox mediator dyes. The solid blue and dotted black traces are essentially superimposable.

DISCUSSION

Here we provide the first structural evidence for the successful design of a binding site for a [4Fe-4S] cluster into a protein

DOI: 10.1021/jacs.5b11734
J. Am. Chem. Soc. 2016, 138, 5262−5270

scaffold, specifically a constituent shell protein of a bacterial organelle. Using a structure-guided approach, we re-engineered the pore of BMC-T1 to selectively incorporate a [4Fe-4S] cluster, i.e., mononuclear Fe, and [2Fe-2S] or [3Fe-4S] clusters were not observed as demonstrated by spectroscopic and structural characterization. The [4Fe-4S] cluster exhibits EPR and redox properties reminiscent of those in low-potential bacterial ferredoxins (Figures 4B and 5A).

The BMC-T1-S55C monomer scaffold is composed of two domains which have complementary roles: the first domain harbors the [4Fe-4S] cluster-binding site (Cys55), while residues within the second domain (Gly155 and Ala157) provide hydrogen-bonding interactions that most likely stabilize the [4Fe-4S] cluster and facilitate its redox reversibility. In most [Fe-S] cluster proteins, the cluster ligands are on the same polypeptide chain; in contrast, each BMC-T1-S55C protomer contributes one-third of the [4Fe-4S] cluster-binding site, which is completed by the trimerization. As observed in other systems, three cysteinate ligands are sufficient for [4Fe-4S] incorporation. The fourth ligand can vary; for example, in radical SAM enzymes, when SAM is present it is the fourth ligand.[45] Similarly to activated aconitase and other dehydratase enzymes,[46,47] a water molecule (or hydroxide ion) completes the primary coordination sphere of the cluster in BMC-T1-S55C (Figure 3B). Therefore, the [4Fe-4S] cluster of BMC-T1-S55C can be considered a hybrid between clusters found in low-potential bacterial ferredoxins (redox and spectroscopic characteristics) and those found in different classes of enzymes (architecture of the cluster).

The reduction potential value of −370 mV at pH 7.5 (Figure 5A) is at the more positive end of the range of −374 to −500 mV reported for bacterial ferredoxins,[48] but well within the range of −700 to +100 mV reported for $[4Fe\text{-}4S]^{2+/+}$ clusters for other [Fe-S] cluster proteins.[49] In comparison to other designed [4Fe-4S] cluster proteins, the reduction potential of BMC-T1-S55C is comparable to the value of −350 mV (at pH 8) reported for the minimal ferredoxin maquette,[50] but significantly more positive than the value reported for the domain-swapped dimer-ferredoxin maquette (DSD-Fdm) of −479 mV (at pH 7.5),[43] as well as the minimal photosystem I F_A- and F_B-maquettes of −440 and −470 mV (at pH 8.3), respectively.[51] The similarity of the reduction potential between BMC-T1-S55C and the minimalist ferredoxin maquette may reflect the degree of solvent exposure of the clusters in both systems, whereas the more negative potential of DSM-Fdm may be due, at least in part, to the burial of the cluster in the hydrophobic core of its three-helix bundle scaffold.[52] Notably, the reduction potential of BMC-T1-S55C is much lower than the value determined for the [4Fe-4S] cluster of PduT from *C. freundii*, +99 mV (at pH 7).[12] This demonstrates that BMC shell proteins can incorporate [4Fe-4S] clusters with a wide range of reduction potentials, suggesting that modifying the environment of the cluster will allow the fine-tuning of the reduction potential of the BMC-T1-S55C [4Fe-4S] cluster to the requirements of the BMC-encapsulated enzymes.

The capacity of the BMC-T1-S55C cluster to function as an electron relay is illustrated by its ability to cycle between oxidized and reduced states without being degraded or oxidatively damaged (Figure 5B). This is in contrast to other designed [4Fe-4S] cluster proteins in which the reduced state is unstable and irreversible.[53] Hydrogen bonding plays an essential role in folding and stability of proteins, and influences the properties of metal centers. Thus, the installation of a hydrogen-bond network is an important consideration in metalloprotein design.[54] As observed in a designed rubredoxin mimic,[55] the presence of second-shell hydrogen-bond interactions between backbone amides (Gly155) and the thiolate ligands of Cys55 (Figure 3B) likely confers stability to the BMC-T1-S55C [4Fe-4S] cluster upon redox cycles. The presence of the hydrogen-bond network in the BMC-T1 scaffold which stabilizes the metal center is an important component of the design. The robustness of the cluster is also illustrated by its resistance to different stressors. For example, BMC-T1-S55C retains a significant amount of intact bound [4Fe-4S] cluster after incubation at 55 °C is used as a first purification step. Preliminary characterization of the stability of the trimer with and without the cluster shows that the holoprotein is more stable in urea than the WT protein (Figure S11).

The BMC-T1-S55C cluster seems somewhat tolerant to oxygen. Indeed, initial purifications of BMC-T1-S55C were performed under aerobic conditions from aerobically grown cultures. The purified protein retained a brown color for a few weeks at 4 °C without bleaching of the chromophore or any precipitation. Another indication of oxygen tolerance is the presence of the intact cluster in the BMC-T1-S55C structure, even though preparing the crystals for data collection required brief exposure to aerobic conditions. However, a combination of UV−vis and EPR spectroscopies suggests that the degradation of the cluster to a [3Fe-4S] form does indeed start shortly after oxygen exposure and continues over time. The [3Fe-4S] is in turn converted to a more stable [2Fe-2S] form (Figure S12). We suspect that in the crystals, during the brief subjection to aerobic conditions prior to data collection, surface proteins likely are in contact with oxygen, but those deeper in the crystal are relatively shielded by other proteins as well as the solvent environment, and so their metal centers are less prone to degradation.

The demonstration that a shell protein can be engineered to bind a [4Fe-4S] cluster not only has implications for BMC engineering but also provides a model for the fundamental understanding of electron transfer across the shell of natural BMCs. There are two BMC shell protein homologues (the BMC-T protein PduT and the BMC-H protein GrpU)[12,17,18] known to bind metal centers, but neither has been structurally characterized with the metal intact; thus, details of the binding modes are unknown. More broadly, our results are of substantial interest for the development of artificial metalloproteins. Because tetranuclear [4Fe-4S] clusters are among the most commonly occurring and versatile redox cofactors, they have been the focus of many studies. For example, minimal maquettes have been used to better understand the chemistry of these cofactors and the influence of the protein environment on their assembly, stabilization, electrochemistry, and physical properties.[50,51,56] Other studies have focused on developing *de novo* designed proteins binding [4Fe-4S] clusters as electron-transfer modules.[43,53] To date, there is only a single report of the successful incorporation of a [4Fe-4S] cluster into a natural protein normally devoid of any cofactors, but the electrochemistry of that cluster demonstrates that it is a high potential iron-sulfur protein accessing the $[4Fe\text{-}4S]^{3+/2+}$ couple.[57] Moreover, there has been no structural evidence for the success of any of the [4Fe-4S] protein designs. Therefore, the use of a BMC shell protein as a scaffold to introduce a [4Fe-4S] cluster also provides a new means to study [Fe-S] cluster properties. Indeed the structure of BMC-T1-S55C will guide

DOI: 10.1021/jacs.5b11734
J. Am. Chem. Soc. 2016, 138, 5262−5270

the manipulation of the protein environment around the cluster, which is critical for fine-tuning its reduction potential to couple with the enzymes encapsulated in the BMC. The ability to transfer electrons into and out of BMC shells opens a new frontier in their applications in synthetic biology.

CONCLUSIONS

In summary, we used a BMC shell protein naturally devoid of any cofactor as a template for structure-based rational design of a [4Fe-4S] cluster-binding site. By a combination of structural and spectroscopic techniques, we showed that the assembly of the cluster in the engineered protein is efficient and specific; 72−74% of the proteins bind a [4Fe-4S] cluster, and no other forms of the cluster were detected. We also showed that the cluster and the ligating cysteine residues are hydrogen-bonded to the main chain of the protein; these interactions likely contribute to the stability of the [4Fe-4S] cluster and facilitate its redox reversibility. It is worth mentioning that this cluster, even though it is exposed to solvent, is relatively resistant to stresses such as high temperature or high concentrations of urea. Finally, the cluster exhibits redox and spectroscopic characteristics of [4Fe-4S] clusters found in low-potential bacterial ferredoxins, while our structural data reveal a binding mode reminiscent of those found in diverse classes of enzymes with only three irons coordinated by cysteine residues. BMC-T1-S55C provides a valuable model to study how a protein scaffold dictates the properties of a [4Fe-4S] cluster and as a proxy for understanding the mechanism of electron transfer across the shell of natural BMCs. Finally, the conversion of a shell protein into an electron-transfer module described in this work provides proof-of-concept of the potential for engineering shell proteins with new functionalities. This study represents a key step in the construction of tailor-made BMCs encapsulating oxidoreductive pathways.

ASSOCIATED CONTENT

Supporting Information

The Supporting Information is available free of charge on the ACS Publications website at DOI: 10.1021/jacs.5b11734.

Experimental details (CD spectroscopy and urea denaturation), Table S1 (data collection and refinement statistics for BMC-T1 and BMC-T1-S55C), and Figures S1−S12 containing additional structural and biochemical analysis, UV−vis, EPR, and CD spectra (PDF)

BMC-T1 and BMC-T1-S55C crystallographic data (CIF)

AUTHOR INFORMATION

Corresponding Author

*ckerfeld@lbl.gov

Present Addresses

◆Max Planck Institute for Terrestrial Microbiology, Marburg, 35043 Germany.

∞Department of Biochemistry, Brandeis University, Waltham, Massachusetts 02453, United States.

Notes

The authors declare no competing financial interest.

ACKNOWLEDGMENTS

This work was supported by the Office of Science of the U.S. Department of Energy DE-FG02-91ER20021 and with infrastructure support from MSU AgBio Research. The Advanced Light Source is supported by the Director, Office of Science, Office of Basic Energy Sciences, of the U.S. Department of Energy under contract no. DE-AC02-05CH11231. Use of the Stanford Synchrotron Radiation Lightsource, SLAC National Accelerator Laboratory, is supported by the U.S. Department of Energy, Office of Science, Office of Basic Energy Sciences under contract no. DE-AC02-76SF00515. B.R.G. acknowledges support from EU FP7 project PEPDIODE (GA 256672). The authors would like to thank Dr. Jonathan Lassila and Susan Bernstein for the construction of the plasmid carrying *hoch_5812*, Prof. John McCracken for the preliminary EPR experiments, and all members of the Kerfeld Lab for helpful discussions.

REFERENCES

(1) Kerfeld, C. A.; Erbilgin, O. *Trends Microbiol.* **2015**, *23*, 22.

(2) Bobik, T. A.; Lehman, B. P.; Yeates, T. O. *Mol. Microbiol.* **2015**, *98*, 193.

(3) Axen, S. D.; Erbilgin, O.; Kerfeld, C. A. *PLoS Comput. Biol.* **2014**, *10*, e1003898.

(4) Klein, M. G.; Zwart, P.; Bagby, S. C.; Cai, F.; Chisholm, S. W.; Heinhorst, S.; Cannon, G. C.; Kerfeld, C. A. *J. Mol. Biol.* **2009**, *392*, 319.

(5) Sagermann, M.; Ohtaki, A.; Nikolakakis, K. *Proc. Natl. Acad. Sci. U. S. A.* **2009**, *106*, 8883.

(6) Tanaka, S.; Kerfeld, C. A.; Sawaya, M. R.; Cai, F.; Heinhorst, S.; Cannon, G. C.; Yeates, T. O. *Science* **2008**, *319*, 1083.

(7) Sutter, M.; Wilson, S. C.; Deutsch, S.; Kerfeld, C. A. *Photosynth. Res.* **2013**, *118*, 9.

(8) Wheatley, N. M.; Gidaniyan, S. D.; Liu, Y.; Cascio, D.; Yeates, T. O. *Protein Sci.* **2013**, *22*, 660.

(9) Kerfeld, C. A.; Sawaya, M. R.; Tanaka, S.; Nguyen, C. V.; Phillips, M.; Beeby, M.; Yeates, T. O. *Science* **2005**, *309*, 936.

(10) Kinney, J. N.; Axen, S. D.; Kerfeld, C. A. *Photosynth. Res.* **2011**, *109*, 21.

(11) Frank, S.; Lawrence, A. D.; Prentice, M. B.; Warren, M. J. *J. Biotechnol.* **2013**, *163*, 273.

(12) Parsons, J. B.; Dinesh, S. D.; Deery, E.; Leech, H. K.; Brindley, A. A.; Heldt, D.; Frank, S.; Smales, C. M.; Lunsdorf, H.; Rambach, A.; Gass, M. H.; Bleloch, A.; McClean, K. J.; Munro, A. W.; Rigby, S. E.; Warren, M. J.; Prentice, M. B. *J. Biol. Chem.* **2008**, *283*, 14366.

(13) Fan, C.; Cheng, S.; Liu, Y.; Escobar, C. M.; Crowley, C. S.; Jefferson, R. E.; Yeates, T. O.; Bobik, T. A. *Proc. Natl. Acad. Sci. U. S. A.* **2010**, *107*, 7509.

(14) Lassila, J. K.; Bernstein, S. L.; Kinney, J. N.; Axen, S. D.; Kerfeld, C. A. *J. Mol. Biol.* **2014**, *426*, 2217.

(15) Lawrence, A. D.; Frank, S.; Newnham, S.; Lee, M. J.; Brown, I. R.; Xue, W. F.; Rowe, M. L.; Mulvihill, D. P.; Prentice, M. B.; Howard, M. J.; Warren, M. J. *ACS Synth. Biol.* **2014**, *3*, 454.

(16) Parsons, J. B.; Lawrence, A. D.; McLean, K. J.; Munro, A. W.; Rigby, S. E.; Warren, M. J. *PLoS One* **2010**, *5*, e14009.

(17) Pang, A.; Warren, M. J.; Pickersgill, R. W. *Acta Crystallogr., Sect. D: Biol. Crystallogr.* **2011**, *67*, 91.

(18) Thompson, M. C.; Wheatley, N. M.; Jorda, J.; Sawaya, M. R.; Gidaniyan, S. D.; Ahmed, H.; Yang, Z.; McCarty, K. N.; Whitelegge, J. P.; Yeates, T. O. *J. Mol. Biol.* **2014**, *426*, 3287.

(19) Beinert, H.; Holm, R. H.; Münck, E. *Science* **1997**, *277*, 653.

(20) Fontecave, M. *Nat. Chem. Biol.* **2006**, *2*, 171.

(21) Capozzi, F.; Ciurli, S.; Luchinat, C. In *Metal Sites in Proteins and Models Redox Centres*; Hill, H. A. O., Sadler, P. J., Thomson, A. J., Eds.; Springer: Berlin Heidelberg, 1998; Vol. *90*, p 127.

(22) Kuchenreuther, J. M.; Grady-Smith, C. S.; Bingham, A. S.; George, S. J.; Cramer, S. P.; Swartz, J. R. *PLoS One* **2010**, *5*, e15491.

(23) Stookey, L. L. *Anal. Chem.* **1970**, *42*, 779.

(24) Kabsch, W. *Acta Crystallogr., Sect. D: Biol. Crystallogr.* **2010**, *66*, 125.

DOI: 10.1021/jacs.5b11734
J. Am. Chem. Soc. 2016, 138, 5262−5270

(25) Winn, M. D.; Ballard, C. C.; Cowtan, K. D.; Dodson, E. J.; Emsley, P.; Evans, P. R.; Keegan, R. M.; Krissinel, E. B.; Leslie, A. G.; McCoy, A.; McNicholas, S. J.; Murshudov, G. N.; Pannu, N. S.; Potterton, E. A.; Powell, H. R.; Read, R. J.; Vagin, A.; Wilson, K. S. *Acta Crystallogr., Sect. D: Biol. Crystallogr.* **2011**, *67*, 235.
(26) McCoy, A. J.; Grosse-Kunstleve, R. W.; Adams, P. D.; Winn, M. D.; Storoni, L. C.; Read, R. J. *J. Appl. Crystallogr.* **2007**, *40*, 658.
(27) Adams, P. D.; Afonine, P. V.; Bunkoczi, G.; Chen, V. B.; Davis, I. W.; Echols, N.; Headd, J. J.; Hung, L. W.; Kapral, G. J.; Grosse-Kunstleve, R. W.; McCoy, A. J.; Moriarty, N. W.; Oeffner, R.; Read, R. J.; Richardson, D. C.; Richardson, J. S.; Terwilliger, T. C.; Zwart, P. H. *Acta Crystallogr., Sect. D: Biol. Crystallogr.* **2010**, *66*, 213.
(28) Emsley, P.; Cowtan, K. *Acta Crystallogr., Sect. D: Biol. Crystallogr.* **2004**, *60*, 2126.
(29) Stoll, S.; Schweiger, A. *J. Magn. Reson.* **2006**, *178*, 42.
(30) Dutton, P. L. *Methods Enzymol.* **1978**, *54*, 411.
(31) Petros, A. K.; Reddi, A. R.; Kennedy, M. L.; Hyslop, A. G.; Gibney, B. R. *Inorg. Chem.* **2006**, *45*, 9941.
(32) Stout, C. D. In *Encyclopedia of Inorganic and Bioinorganic Chemistry*; John Wiley & Sons, Ltd: Hoboken, NJ, 2011; accessed December 17, 2015.
(33) Giastas, P.; Pinotsis, N.; Efthymiou, G.; Wilmanns, M.; Kyritsis, P.; Moulis, J. M.; Mavridis, I. M. *JBIC, J. Biol. Inorg. Chem.* **2006**, *11*, 445.
(34) Mitra, D.; George, S. J.; Guo, Y.; Kamali, S.; Keable, S.; Peters, J. W.; Pelmenschikov, V.; Case, D. A.; Cramer, S. P. *J. Am. Chem. Soc.* **2013**, *135*, 2530.
(35) Herskovitz, T.; Averill, B. A.; Holm, R. H.; Ibers, J. A.; Phillips, W. D.; Weiher, J. F. *Proc. Natl. Acad. Sci. U. S. A.* **1972**, *69*, 2437.
(36) Fukuyama, K. In *Encyclopedia of Inorganic and Bioinorganic Chemistry*; John Wiley & Sons, Ltd: Hoboken, NJ, 2011; accessed December 17, 2015.
(37) Sweeney, W. V.; Rabinowitz, J. C. *Annu. Rev. Biochem.* **1980**, *49*, 139.
(38) Lippard, S. J.; Berg, J. M. In *Principles of Bioinorganic Chemistry*; University Science Books: Mill Valley, CA, 1994.
(39) Mayhew, S. G. *Eur. J. Biochem.* **1978**, *85*, 535.
(40) Lanz, N. D.; Grove, T. L.; Gogonea, C. B.; Lee, K. H.; Krebs, C.; Booker, S. J. *Methods Enzymol.* **2012**, *516*, 125.
(41) Guigliarelli, B.; Bertrand, P. *Adv. Inorg. Chem.* **1999**, *47*, 421.
(42) Cleland, W. W. *Biochemistry* **1964**, *3*, 480.
(43) Roy, A.; Sommer, D. J.; Schmitz, R. A.; Brown, C. L.; Gust, D.; Astashkin, A.; Ghirlanda, G. *J. Am. Chem. Soc.* **2014**, *136*, 17343.
(44) Rouault, T. *Iron-Sulfur Clusters in Chemistry and Biology*; De Gruyter: Berlin, 2014.
(45) Broderick, J. B.; Duffus, B. R.; Duschene, K. S.; Shepard, E. M. *Chem. Rev.* **2014**, *114*, 4229.
(46) Robbins, A. H.; Stout, C. D. *Proc. Natl. Acad. Sci. U. S. A.* **1989**, *86*, 3639.
(47) Imlay, J. A. *Mol. Microbiol.* **2006**, *59*, 1073.
(48) Moura, J. J.; Macedo, A. L.; Palma, P. N. *Methods Enzymol.* **1994**, *243*, 165.
(49) Johnson, M. K.; Smith, A. D. In *Encyclopedia of Inorganic and Bioinorganic Chemistry*; John Wiley & Sons, Ltd: Hoboken, NJ, 2011; accessed December 17, 2015.
(50) Gibney, B. R.; Mulholland, S. E.; Rabanal, F.; Dutton, P. L. *Proc. Natl. Acad. Sci. U. S. A.* **1996**, *93*, 15041.
(51) Antonkine, M. L.; Koay, M. S.; Epel, B.; Breitenstein, C.; Gopta, O.; Gartner, W.; Bill, E.; Lubitz, W. *Biochim. Biophys. Acta, Bioenerg.* **2009**, *1787*, 995.
(52) Saridakis, E.; Giastas, P.; Efthymiou, G.; Thoma, V.; Moulis, J. M.; Kyritsis, P.; Mavridis, I. M. *JBIC, J. Biol. Inorg. Chem.* **2009**, *14*, 783.
(53) Grzyb, J.; Xu, F.; Weiner, L.; Reijerse, E. J.; Lubitz, W.; Nanda, V.; Noy, D. *Biochim. Biophys. Acta, Bioenerg.* **2010**, *1797*, 406.
(54) Yu, F.; Cangelosi, V. M.; Zastrow, M. L.; Tegoni, M.; Plegaria, J. S.; Tebo, A. G.; Mocny, C. S.; Ruckthong, L.; Qayyum, H.; Pecoraro, V. L. *Chem. Rev.* **2014**, *114*, 3495.
(55) Nanda, V.; Rosenblatt, M. M.; Osyczka, A.; Kono, H.; Getahun, Z.; Dutton, P. L.; Saven, J. G.; DeGrado, W. F. *J. Am. Chem. Soc.* **2005**, *127*, 5804.
(56) Hoppe, A.; Pandelia, M. E.; Gartner, W.; Lubitz, W. *Biochim. Biophys. Acta, Bioenerg.* **2011**, *1807*, 1414.
(57) Coldren, C. D.; Hellinga, H. W.; Caradonna, J. P. *Proc. Natl. Acad. Sci. U. S. A.* **1997**, *94*, 6635.

DOI: 10.1021/jacs.5b11734
J. Am. Chem. Soc. 2016, 138, 5262−5270